

THE DOUBLE EAGLE SPACE EXPERIMENT (DESE) BEAMLINE DESIGN†

A. M. M. Todd, D. Berwald, D. L. Bruhwiler, S. L. Mendelsohn, C. C. Paulson, M. F. Reusch and P. Walstrom,
Grumman Research and Development Center, 4 Independence Way, Princeton, New Jersey 08540, USA,

and

A. Jason, R. Kraus, W. P. Lysenko, C. T. Mottershead, F. Neri, R. Sander, R. Shafer and E. A. Wadlinger,
Los Alamos National Laboratory, Los Alamos, New Mexico 87545, USA.

Abstract

The beamline design for the Double Eagle Space Experiment (DESE) is described. DESE seeks to map the lunar surface material composition using an active particle beam probe. The 425 MHz, 11.8 m straight beamline delivers a 13 mA, 5.11 MeV neutral hydrogen beam with an rms divergence of $\sim 40 \mu\text{rad}$. We have studied the beam propagation through the output optics components to the lunar surface and find an adequate return signal for the DESE mapping mission.

1. Introduction

The Double Eagle Space Experiment (DESE) is a 425 MHz, 11.8 m straight beamline that can be packaged on a Russian Proton launch vehicle to deliver a 13 mA, 5.11 MeV neutral hydrogen beam with an rms divergence of $\sim 40 \mu\text{rad}$. This twelve month lunar mission proposes to use a joint Russian and United States spacecraft to map the lunar surface material content at specific sites using PIXE (Proton Induced X-ray Emission) measurements. The output energy choice was driven by signal to noise ratio trades for the return signal. Fig. 1 shows the DESE spacecraft, while Table 1 gives a top level parameter summary of the beamline components. Table 1 values in parentheses are either projected RF unit sizes or embedded component lengths.

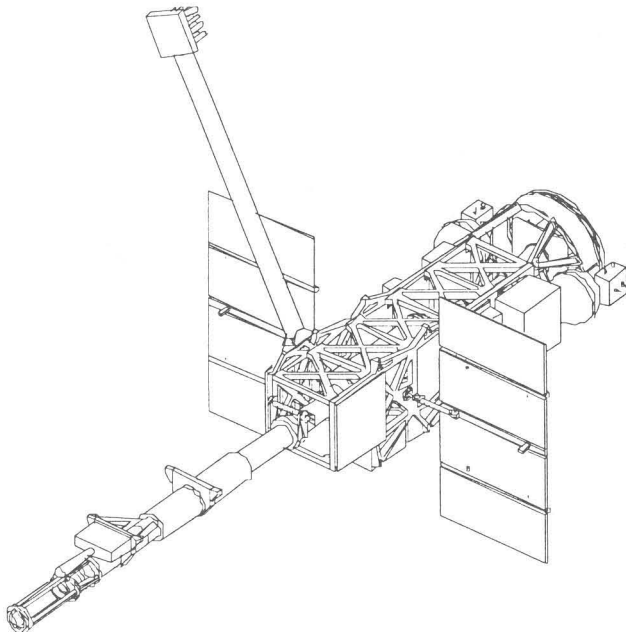


Fig. 1 The DESE spacecraft.

† Supported by United States Army Strategic Defense Command under Contract No. DASG60-90-C-0103 and by the Grumman Aerospace Corporation

TABLE 1
DESE Component Parameter Summary

Component	Energy (MeV-In)	Length (m)	Power (kW)	Heat (kW)
Injector	0.035	1.200	70	69
RFQ	2.000	1.746	235 (300)	185
DTL	5.110	1.871	255 (300)	174
Telescope	5.110	4.300	~ 0	17
$\delta p/p$ Compactor	5.110	(0.07)	36 (60)	36
Steerer	5.110	(0.750)	< 1	6
WAFFOG	5.110	0.750	~ 0	6
Neutralizer	5.110	1.467	~ 0	~ 0
Electron Collector	5.110	0.500	~ 0	~ 0
TOTALS	5.110	11.834	587 (660)	493

2. Accelerator Elements

Since the injector, accelerator designs are largely conventional, we will concentrate on two unusual aspects of the DTL design. The injector is a cesiated LBL-design RF volume source engineered by AEA Technologies and Marconi plc. for 35-kV extraction. Space operation drives the RFQ design to minimum power, which requires a narrow aperture, and to minimum length, which requires aggressive modulation ramping, to yield the desired performance. The design, which follows the principles used for the SSC RFQ [1] to produce a 2.0 MeV beam, has excellent performance, but requires a very narrow machining tool for the 0.47 cm minimum longitudinal vane radius of curvature.

The DTL accelerates the beam at near constant $\{E_0 T / \beta\}$ to 5.11 MeV. This linear field-ramped $\beta\lambda$ FO-DO device has 32 cells, most at a synchronous phase of -27° . Direct DTL to RFQ coupling is employed, which leads to reduced beamline length and power requirements. By phasing the first DTL cell at -90° to act as a buncher for longitudinal matching, and using the first four DTL drift tube permanent magnet quadrupoles (PMQ) for transverse matching, a good relatively current-independent match can be achieved, as illustrated by the upper TRACE 3-D [2] beam envelopes of Fig. 2. The upper and lower box heights are respectively 5, 150 mm for the transverse beam envelopes, and $35^\circ, 60^\circ$ for the longitudinal phase spreads. These plots utilize standard TRACE 3-D envelope conventions.

Noting that there is virtually no length available for pre-compaction drifting, we stretch the phase and energy of DTL bunches prior to 425 MHz compaction by utilizing $+27^\circ$ phasing in the last four DTL cells. This behavior is indicated in both TRACE 3-D envelopes of Fig. 2, where the increasing phase in the tail of the DTL is evident before the compactor, located just after the quadruplet eyepiece, flattens the longitudinal envelope. The output momentum spread achieved in this manner is $\delta p/p \sim 8.5 \times 10^{-4}$, which is sufficient to reduce the critical output optics chromatic aberration to levels consistent with mission requirements.

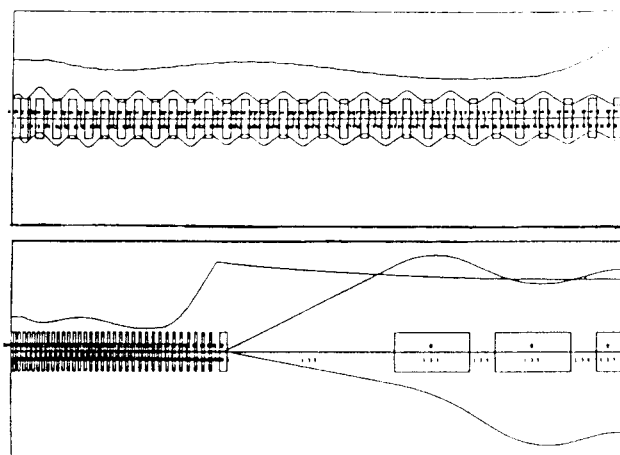


Fig. 2 TRACE 3-D beam envelopes for direct DTL/RFAQ matching (left-upper), positive DTL phasing (right-upper), and expansion/compaction in optical elements (right-lower).

Fig. 3 demonstrates that satisfactory beam dynamics performance, as measured by transverse (normalized to the RFQ input) and longitudinal emittance (normalized to the RFQ output), is achieved through the accelerator components. Cell number, which distorts the length but highlights variations, is used for the horizontal scale. The theoretical RFQ and DTL transmissions are 76.3% and 100% respectively. The low value for the RFQ is a result of a requirement change that increased the input RFQ current above the original design value. The RFQ design should now be revised to recover an acceptable transmission. At the same time, design variants which improve the longitudinal radius machinability without penalizing either the output brightness or the power consumption and geometrical envelope, should be studied.

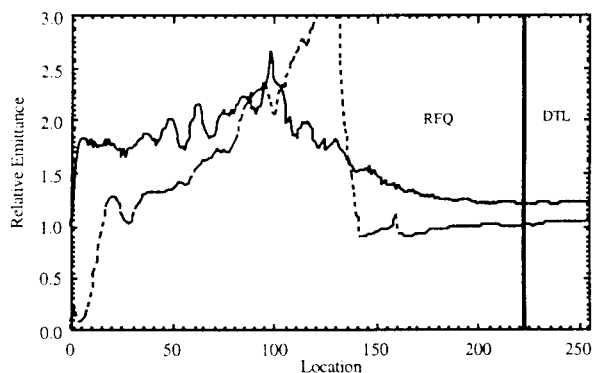


Fig. 3 Relative accelerator longitudinal (dotted) and transverse (solid) emittance growth.

3. Optics Elements

The components of the quadruplet eyepiece and the 4.3 m long Permanent Magnet Quadrupole (PMQ) triplet objective telescope are summarized in Table 2. The PMQs in the objectives consist of 0.25 m sections, each with a built-in Octupole (PMO) corrector component. The octupoles serve to cancel third-order-aberrations while minimizing fifth-order increments. The steerer magnet lies inside the last 0.75 m of the telescope and these various embedded lengths are shown in

parentheses. The PMQ strengths are given in T/m, the PMO strengths in T/m³, and the compactor voltage (including the transit-time factor) in MV.

The quadruplet eyepiece begins with a brief extension of the DTL lattice in the first two PMQs to allow pre-compaction beam correlation development. Together, the last two quadrupoles of the eyepiece and the triplet objective control the beam focus and magnification in both transverse planes (yielding a 5 cm rms radius round beam focused at infinity), and match the maximum beam excursion in these planes so as to minimize the required beam pipe radius. A dipole trim corrector package is included after the eyepiece, and three multipole trim corrector packages which include octupole and both regular and skew quadrupole and sextupole components, are positioned within the objectives. These corrector packages are required to maintain beam focus and centroid location in the presence of beamline vibration, torsion and beam steering, as well as to correct for second-order geometric aberrations induced by the steering magnet and by temperature variations in the PMQs.

TABLE 2
DESE Optics Component Summary

Component	Length (mm)	Strength (T/m ³ , MV)	Bore (mm)
DTL Exit 1/2 PMQ	12.5	168.50	10.0
Drift	48.0	--	--
Eyepiece PMQ (#1)	25.0	-168.50	10.0
Drift	48.0	--	--
Eyepiece PMQ (#2)	25.0	168.50	10.0
Drift	48.0	--	--
Eyepiece PMQ (#3)	25.0	-38.00	10.0
Drift	5.0	--	--
Compactor (-90°)	70.0	0.226 (E ₀ TL)	15.0
Drift	5.0	--	--
Eyepiece PMQ (#4)	75.0	105.59	10.0
Drift	50.0	--	--
Dipole Trim	50.0	Not Specified	20.0
Drift (Throw)	1576.0	--	--
2σ Elliptical Scraper	--	--	--
Trim Package (#1)	(400.0)	Not Specified	250.0
Objective PMQ (#1)	750.0	-0.43004	350.0
Objective PMO (#1a)	(250.0)	2.8779	350.0
Objective PMO (#1b)	(250.0)	2.6853	350.0
Objective PMO (#1c)	(250.0)	-2.8822	350.0
Drift	250.0	--	--
Trim Package (#2)	(400.0)	Not Specified	250.0
Objective PMQ (#2)	750.0	0.45639	350.0
Objective PMO (#2a)	(250.0)	-2.8822	350.0
Objective PMO (#2b)	(250.0)	2.8638	350.0
Objective PMO (#2c)	(250.0)	1.6676	350.0
Drift	250.0	--	--
Trim Package (#3)	(400.0)	Not Specified	250.0
Objective PMQ (#3)	250.0	-0.50247	350.0
Objective PMO (#3a)	(250.0)	-2.8814	350.0
Steering Magnet	(750.0)	--	250.0

The divergence budget of Table 3 illustrates that the largest contribution is intrinsic emittance, followed closely by telescope chromatic aberrations. Contributions from the neutralizer and from geometric aberrations are much smaller in magnitude, but still significant. In particular, these contributions add long tails to the initially Gaussian momentum distribution. Such tails grossly distort rms divergence calculations, so it became necessary to use another

divergence measure, $\theta_{1/2}$, in order to obtain reliable performance assessments. $\theta_{1/2}$ is defined to be the half angle of the cone which encompasses the trajectories of 50% of the beam leaving the telescope. The various divergence contributions add in quadrature (not including the effects of steering) to yield the total of 47.0 μrad , which corresponds to $\theta_{\text{rms}} \sim 40 \mu\text{rad}$ if the tails of the distribution are ignored. Momentum compaction minimized chromatic aberrations, while PMOs were positioned to control geometric aberrations. It was found that space charge affected the PMQ and compactor but not the PMO settings implying that the space charge effects are largely linear.

TABLE 3
DESE Divergence Budget

Contribution	Divergence $\theta_{1/2}$ (μrad)
Intrinsic Emittance	33.4
Telescope Chromatic	27.7
Neutralizer	12.5
Geometric	13.0
Steering at 0.25°	(4.4)
TOTAL	47.0

The $\pm 0.25^\circ$ two-axis steering magnet has a 50 cm winding length and 25 cm fringe field clearance from both the objective and the Wire And Fluorescent Fiber Over Grid (WAFFOG) beam direction sensor. Coils to null stray dipole fields to ≤ 0.05 G are required over the entire optics length to eliminate transverse deflections.

The WAFFOG wires scrape $\sim 3\%$ (0.6 mA) of the beam to provide beam direction information. Coupled with an $\sim 15\%$ scrape-off in the telescope and a 40% gas neutralizer efficiency, the beamline is projected to eventually propagate ~ 13 mA neutral current beam towards the lunar surface. The WAFFOG is required to provide focus data to $\sim 20 \mu\text{rad}$ because of the ± 2 K permissible thermal range for holding PMQ focus strength, and beam direction data to $\sim 10 \mu\text{rad}$ for pointing requirements. Because of the low stripping line density required by the 5 MeV output beam, DESE uses a ring gas jet rather than a foil neutralizer. Electrons from the neutralization process are collected to maintain spacecraft neutrality and as a measure of neutralization efficiency.

4. Lunar Propagation

The DESE particle beam must traverse a distance $L \geq 50$ km from the platform to the lunar surface. Charged particles will be deflected by the $B_s \sim 6 \times 10^{-9}$ T solar magnetic field, which dominates the earth's field as well as any fields of lunar origin. The magnetic rigidity of 5.11 MeV hydrogen is $B_p = 0.327$ T-m, and the transverse deflection (assuming the worst case where B_s is perpendicular to the propagation direction of the beam) is $\Delta x \approx B_s L^2 / B_p \sim 45$ m.

If the gas neutralizer is configured to yield a macroscopically neutral beam (rather than to maximize the yield of H^0), the 30 mA H^- beam is separated into 9 mA H^- , 9 mA H^+ and 12 mA H^0 . The H^- and H^+ beams will be steered in opposite directions by the solar field, and will expand somewhat due to space charge effects, while the H^0 beam will maintain its low divergence and remain undeflected. This simple scenario has been simulated and the projected beam at

the lunar surface is shown in Fig. 4. If a charged proton beam were utilized, the centroid location of the return signal has an ~ 100 m uncertainty and spacecraft charging becomes an issue, perhaps requiring the inclusion of an electron gun. For these reasons, the present accelerated H^- beam was adopted since the neutral component provides a clear central reference, spacecraft charging can be avoided and yet the return signal of all three beams can still be utilized by the detectors.

The beam transport scenario described above is pessimistic since it neglects the attractive electrostatic forces between the H^- and H^+ beams. Therefore, one would not necessarily expect to see three distinct spots as is shown in Fig. 4; rather, the figure is intended to indicate that, for a worst case 50 km scenario, one would expect the beam footprint to lie within a 100 m circle. An optimistic scenario has been considered previously [4], in which the two charged beams are treated as rigid cylinders. In this limit, the electrostatic attraction between the two cylinders easily overcomes the magnetic force trying to separate them. The true situation will lie somewhere between these two limits, with an accurate simulation requiring the use of a PIC code.

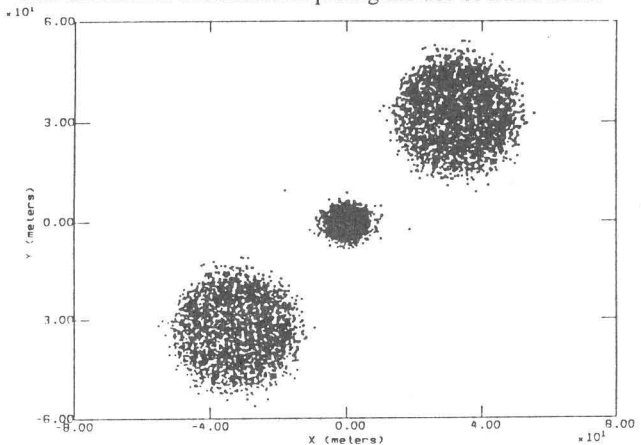


Fig. 4 Nominal beam footprint at the lunar surface.

5. Conclusions

The preliminary beamline design of a 5 MeV accelerator space experiment designated DESE, adapted for launch within Russian Proton launch vehicle payload constraints, has been completed. Experimental scenarios have been developed for this design, whose simulations show that the prescribed lunar mapping mission can be performed.

6. References

- [1] T. S. Bhatia, J. H. Billen, A. Cucchetti, F. W. Guy, G. Neuschaefer and L. M. Young, "Beam Dynamics Design of an RFQ for the SSC Laboratory", *Proceedings of the 1991 Particle Accelerator Conference*, IEEE 91CH3038-7 3 (1991) 1884.
- [2] K. R. Crandall, "TRACE 3-D Documentation", 2nd Edition edited by D. P. Rusthoi, Los Alamos report # LA-UR-90-4146 (1990).
- [3] D. L. Bruhwiler, M. F. Reusch, J. Rathke, I. S. Lehrman and A. M. M. Todd, "Detailed High-Current Beam Optics Design for Ions and Electrons", *these Proceedings*.
- [4] J. P. Blewett, "Neutral Beams including Neutral Atoms, Positive Ions and Negative Ions", Brookhaven National Laboratory report # NPB-120 (1984).